Vis/NIR Hyperspectral Imaging for Detection of Hidden Bruises on Kiwifruits

Qiang LÜ[1,2], Ming-jie TANG[1], Jian-rong CAI[1], Jie-wen ZHAO[1] and Saritporn VITTAYAPADUNG[3]

[1]School of Food and Biological Engineering, Jiangsu University, Zhenjiang, Jiangsu, P.R. China; [2]School of Information Science and Engineering, Henan University of Technology, Zhengzhou, Henan, P.R. China; [3]FAME Laboratory, Department of Mechanical Engineering, Chiang Mai University, Chiang Mai, Thailand

Abstract

Lü Q., Tang M.-J., Cai J.-R., Zhao J.-W., Vittayapadung S. (2011): **Vis/NIR hyperspectral imaging for detection of hidden bruises on kiwifruits**. Czech J. Food Sci., **29**: 595–602.

It is necessary to develop a non-destructive technique for kiwifruit quality analysis because the machine injury could lower the quality of fruit and incur economic losses. Bruises are not visible externally owing to the special physical properties of kiwifruit peel.We proposed the hyperspectral imaging technique to inspect the hidden bruises on kiwifruit. The Vis/NIR (408–1117 nm) hyperspectral image data was collected. Multiple optimal wavelength (682, 723, 744, 810, and 852 nm) images were obtained using principal component analysis on the high dimension spectral image data (wavelength range from 600 nm to 900 nm). The bruise regions were extracted from the component images of the five waveband images using RBF-SVM classification. The experimental results showed that the error of hidden bruises detection on fruits by means of hyperspectral imaging was 12.5%. It was concluded that the multiple optimal waveband images could be used to constructs a multispectral detection system for hidden bruises on kiwifruits.

Keywords: *Actinidia deliciosa*; principal component analysis; support vector machine

Kiwifruit, which is nutritious and sweet in flavour, is one of the most favourite fruits for the population. However, excessive mechanical loading and stress cause injuries to kiwifruits during the processes of harvest, transport, handling, and storage. Severely injured fruits (i.e. broken, and smashed) are easily identified and removed. However, some injuries often cause internal physical hidden bruises under the kiwifruit peel. The bruises lower the quality of the fruits and cause significant economic losses because such fruits easily ferment, rot, or get mildewed, and infect other normal fruits during the storage. Bruised kiwifruits have become a great and growing concern to the kiwifruit industry. So, it is necessary to develop a detection technique for distinguishing the bruised kiwifruits from the normal fruits.

In the past two decades, a number of techniques have been researched for an automated non-destructive detection of fruits and vegetables quality. Computer vision (visible imaging) has been used for many tasks such as the shape classification, defect detection, quality grading, and variety classification (Leemans *et al*. 1998; Cao *et al*. 1999; Paulus *et al*. 1999; Brosnan *et al*. 2004; Throop *et al*. 2005). X-ray imaging has

Supported by the National Natural Science Foundation of China, Grant No. 30771243.

been used to inspect internal quality, such as water core, bruise of apple (Shahin *et al*. 1999, 2002b; Kim *et al*. 2000), weevil-infested mango (Thomas & Kannan 1995), and rotten onion (Shahin *et al*. 2002a), etc.

In the recent years, hyperspectral imaging has been investigated for the estimation of quality and safety of poultry (Liu *et al*. 2003; Park *et al*. 2006, 2007), fruits (Lu *et al*. 1999; Lu 2003; Mehl *et al*. 2004; Xing & Baerdemaeker 2005; Xing *et al*. 2005, 2007; Noh & Lu 2007; Qin *et al*. 2009), vegetables (Liu *et al*. 2005; Ariana *et al*. 2006), and milk (Qin & Lu 2007). Lu *et al*. (1999) have studied hyperspectral imaging for detecting bruises on three cultivars of apples in the spectral region between 450 nm and 900 nm. Lu (2003) has studied NIR (900–1700 nm) hyperspectral imaging for identifying and segregating both new and old bruises on the normal tissue of apple with InGaAs detector. This study has shown that the spectral region of 1000–1340 nm is the most appropriate for the apple bruises detection.

To our knowledge, no research has been conducted for the non-destructive detection of hidden bruises on kiwifruits. Because of the toughness and taupe of kiwifruit peel, the bruise can not be expressed on the peel. It is difficult to be detected by human inspectors or visible imaging. The fruit juice quickly gathers in the bruise regions after the fruit tissue has been damaged. Because the water content of kiwifruit is high, the qualitative difference between the bruise regions and normal regions is not sufficient to distinguish the defective fruits using X-ray imaging.

The hyperspectral imaging combines conventional spectroscopy and imaging techniques to acquire both spectral and spatial information from the object examined. The overall objective of this research was to investigate the potential of using hyperspectral imaging in visible and near-infrared (Vis/NIR) regions (408–1117 nm) for the detection of bruises on kiwifruits. The specific objectives were to:

– Develop a Vis/NIR hyperspectral imaging system covering the spectral region from 408 nm to 1117 nm for the bruise detection.
– Develop computer algorithms to identify and segregate the bruised tissue fom the normal tissue of kiwifruit.
– Identify several important wavelengths that can be utilised for the future solution of detecting bruise in real time by multispectral imaging.

MATERIAL AND METHODS

Sample preparation. The tested kiwifruit cv. Zhonghua was produced in Zhouzhi County, Shaanxi Province, China. Two hundred non-bruised kiwifruits were manually selected through visual and touch inspection, and purchased from a local Zhenjiang supermarket in October, 2008. The kiwifruits were randomly divided into two groups of 100 samples each. The first group was used as control (normal kiwifruits); another one contained bruised kiwifruits damaged artificially. The samples of both groups were stored at room temperature (25 ± 1°C) for 24 h before the measurement. There were no obvious bruise features on the kiwifruits surfaces detected by visual inspection. When hyperspectral image data were collected, all fruits were peeled to detect the presence of bruises. Colour images of bruised kiwifruits before and after peeling are shown in Figure 1.

Hyperspectral image data acquisition. The scheme of the hyperspectral imaging system, developed for this study, is shown in Figure 2. The system is composed of three major units. The imaging unit consists of a complementary metal oxide semiconductor (CMOS) camera (BCi4-U-M-20-LP, Vector International, Leuven, Belgium), and an imaging spectrograph (ImSpector V10E, Specim Spectral Image Ltd., Oulu, Finland) coupled with a 23 mm focal length C-Mount zoom lens. The ImSpector spectrograph contains a fixed-size internal slit to define the field of view for the spatial line and a prism-grating-prism (PGP) system for the separation of the spectra along the spatial line. The lighting unit is a DC regulated light source from a 150W tungsten halogen lamp (DC-950A, Dolan-Jenner Industries Inc., Boxborough, USA) delivered through dual fiber optic light lines (QDF3948, Dolan-Jenner Industries Inc., Boxborough, USA). The conveyer unit consists of a motorised translation stage (TSA200-A, Zolix Instruments Co., Beijing, China), and a motion controller (SC300-1A, Zolix Instruments Co., Beijing, China).

The hyperspectral imaging system is a push broom and line-scan based imaging system. The kiwifruit is put on the translation stage in this system to begin the data acquisition. The CMOS camera is a linear array detector with a 1280 by 1 pixel resolution in a scanned line. The camera and spectrograph have been used to scan the fruit line-by-line as the translation stage moved the fruit

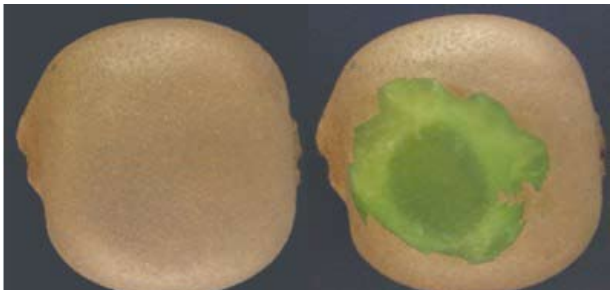

(a) (b)

Figure 1. Colour images of bruised kiwifruit obtained before (a) and after (b) peeling of skin

through the field of view of the optical system. The spectral range of the hyperspectral camera is from 408 nm to 1117 nm with 0.69 nm spectral intervals, which has resulted in 1024 spectral bands. After finishing the scans on one entire kiwifruit, the spatial-by-spectral matrices are combined to construct a three-dimensional (3D, 1280 × 500 × 1024) spatial and spectral data space.

Image calibration. The hyperspectral images of the kiwifruits were first calibrated with a white and a dark references using the following equation:

$$R = \frac{I - B}{W - B} \quad (1)$$

where:

R – relative corrected reflectance image

I – original hyperspectral image of kiwifruit

B – dark image (approximately 0% reflectance) recorded by turning off all light sources and covering the lens with a black cap

W – white image obtained by a reference panel (Spectralon, Labsphere Inc., North Sutton, USA) with approximately 99% reflectance

The representative calibrated reflectance spectra (408–1117 nm), which were obtained from this hyperspectral imaging system, are demonstrated in Figure 3.

Data reduction. Figure 3 shows the average spectral profiles of different regions (50 × 50 pixels, three normal regions (No. 1–3), and three bruise regions (No. 4–6)) of a single sample. According to Figure 3, the spectral profiles of kiwifruit were very close to one another in the spectral regions below 600 nm and over 900 nm, and there was a high noise level over 1000 nm. Therefore, the spectral region of 600–900 nm was used in the next analysis, thus providing 580 spectral bands in the spectral region.

In order to remove the noise and redundant data, the average of every five pixels after calibration in the spectral dimension was used in the subsequent analyses. 520 pixels from 281 to 800 were selected in the horizontal (X-axis) direction to ensure the kiwifruit image integration, thus the 3D data cube was 520 × 500 × 88, which greatly decreased the dataset. Before further data processing, the background of the image was removed by the simple thresholding method. A mask was built from the image at 650 nm when the threshold was set at 0.09. The mask was applied to obtain the area of kiwifruit from the hyperspectral image data. The resultant images were further processed by the principal components analysis (PCA) and support vector machine (SVM).

Principal component analysis. PCA is a very effective data reduction technique for spectroscopic data. It summarises the data by forming new variables, which are linear composites of the original variables. In this study, PCA was performed to reduce spectral dimensionality and enhance image features. A large amount of hyperspectral images was obtained, so PCA was used to find several dominant spectral band images (i.e. optimal band

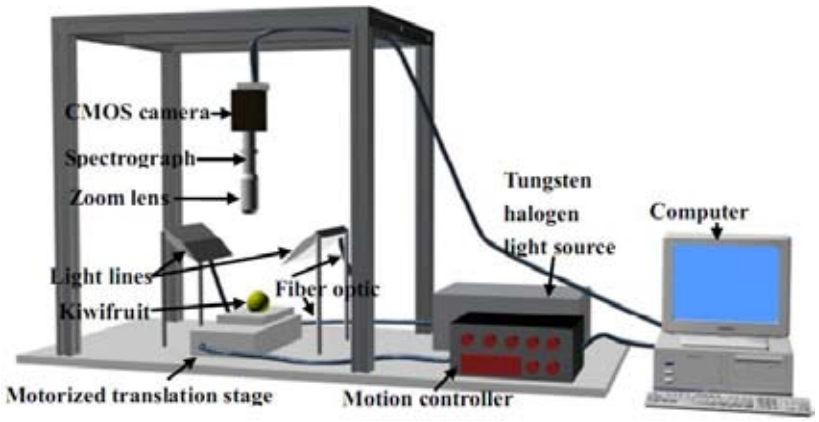

Figure 2. Sketch of the hyperspectral imaging system

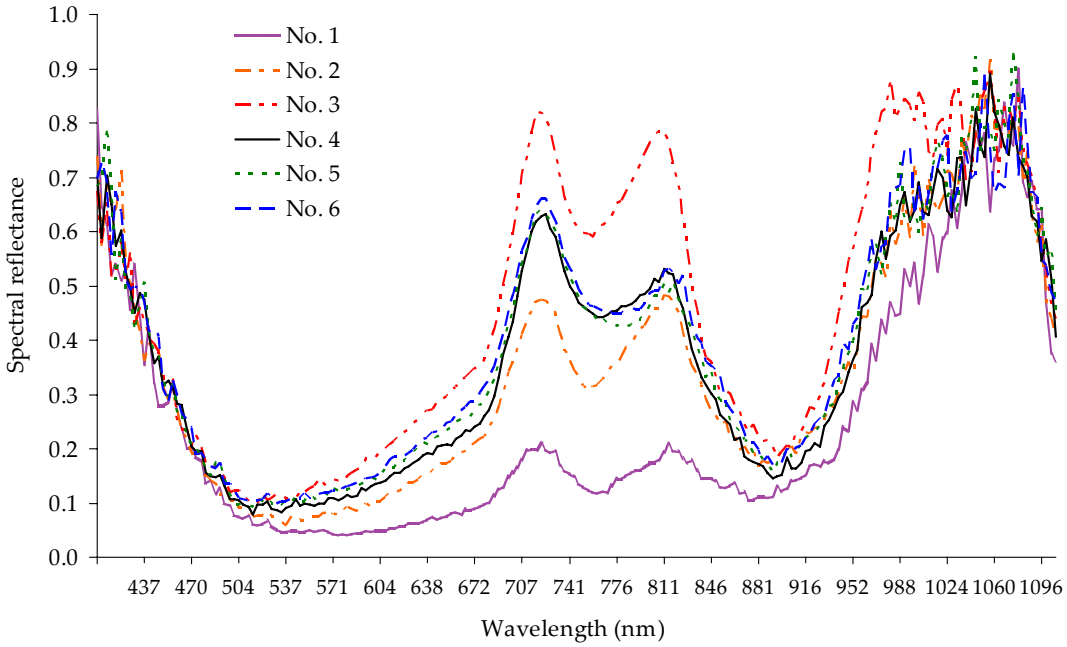

Figure 3. Spectral profiles (408–1117 nm) of kiwifruit sample

images) in order to minimise the amount of the data without sacrificing the detection results.

Support vector machine. Support vector machine (SVM) is based on statistical learning theory (SLT) as proposed by Vapnik and Chervonenkis (Vapnik 1998). The main idea of SVM is to separate the classes with a hyperplane surface so as to maximise the margin between them. Following the structural risk minimisation (SRM) principle, SVM can effectively overcome over-fitting and under-fitting problems and provides a greater generalisation ability (Byun & Lee 2002; Guo *et al*. 2006; Qian *et al*. 2010). In this study, the radial basic function SVM (RBF-SVM) classifier (Guo *et al*. 2006) was used to segment the bruise region on kiwifruit.

Software. For hyperspectral image acquisition, SpectralCube (AutoVision Inc., Mojave, USA) was used. All data processing and analysis procedures described above were performed using the Environment for Visualizing Images (ENVI) V.4.5 (Research Systems Inc., Fort Collins, USA) and MVTec Halcon 8.0 (MVTec Software GmbH, Munich, Germany) for Windows XP.

RESULTS AND DISCUSSION

PCA on the hyperspectral data

Firstly, the hyperspectral data were preprocessed as described above: reflectance calibration, data reduction, and background removal. Afterwards, PCA was performed on the hyperspectral data (600–900 nm) of each kiwifruit, and hence the large amount of hyperspectral data of each fruit was represented by several principal component images. The top five principal component images (PC1 to PC5) are shown in Figure 4. According to the visual inspection, the PC1 mainly represents

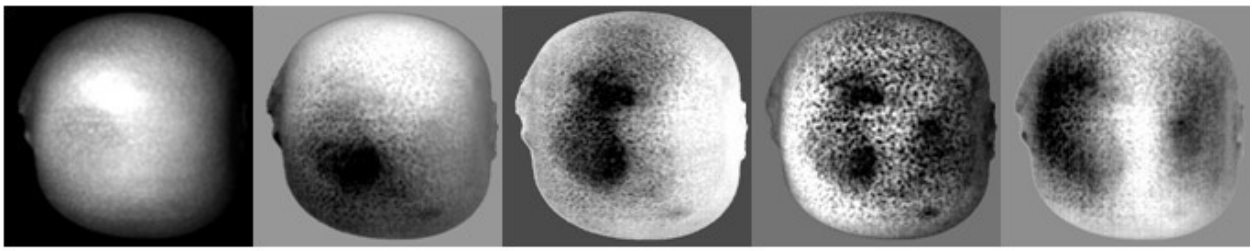

Figure 4. Principal component score images based on the wavelength region of 600–900 nm

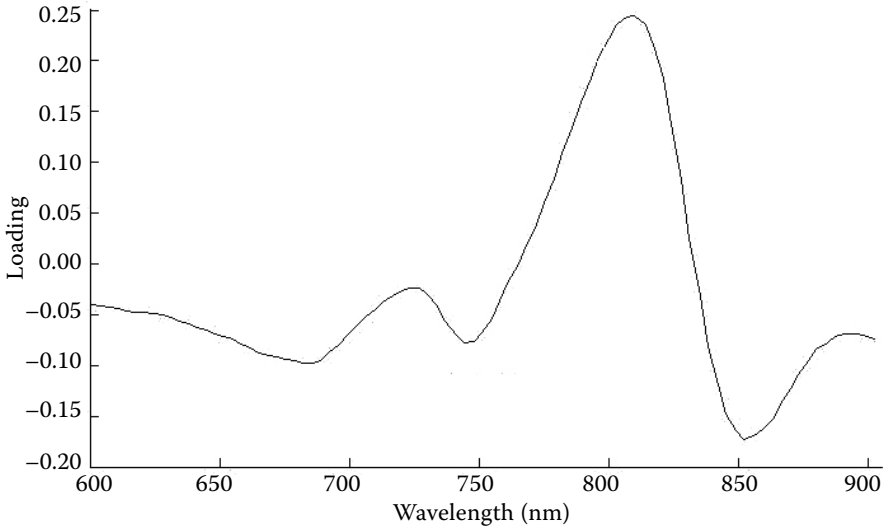

Figure 5. PCA loading plot of PC2 in the region of 600–900 nm

the grey value of the kiwifruit, while the PC2 demonstrates a more extensive volume of information about the fruit quality. The bruise region could be clearly identified in the PC2 image.

PCA at selected optimal wavebands

The main purpose of the study was to select several most suitable wavelengths for discriminating bruises from normal tissue using a multi-spectral imaging system. Based on the results obtained from the hyperspectral images, a set of wavelengths can be selected for multispectral imaging system. To get five principal components, at least five original variables are needed. Therefore, according to the loadings of PC2 (Figure 5), five wavelengths 682 nm, 723 nm, 744 nm, 810 nm, and 852 nm were selected, respectively. The images obtained at five optimal wavelengths are shown in Figure 6. The PCA procedure was then performed at the selected optimal wavelengths instead of the spectral images ranged from 600–900 nm. The resultant multispectral PCA images (Figure 7) gave results similar to those obtained from the whole selected wavelength region.

Segmentation of bruise region

In the reports of Mehl *et al*. (2004), Xing *et al*. (2005, 2007), Ariana *et al*. (2006), and Qin *et al*. (2008, 2009), owing to the obvious differences between the abnormality (i.e. bruise, rot, scab, canker, greasy spot, insect damage) regions and those of normal tissue of fruit (i.e. apple, cucumber, citrus) at some selected wavelength images, the former regions were segmented from these images using some appropriate methods. The waveband images of kiwifruit (Figure 6) revealed no obvious contrast between the bruise region and normal tissue. It was difficult to segment the bruise regions from the images using common image segmentation methods. Therefore, the bruise region was segmented using SVM based on the PCA images (Figure 7) obtained from the selected multiple wavelengths in the next processing.

In order to select the optimum classifier using SVM algorithm for identifying the bruise region of kiwifruit, regions of interest (ROIs) were generated from the bruise area and normal area, and their corresponding spectra of each ROI were

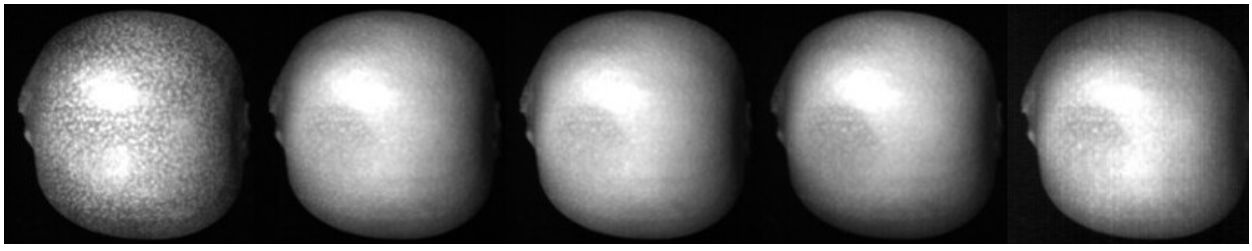

Figure 6. Images obtained at the selected wavelengths

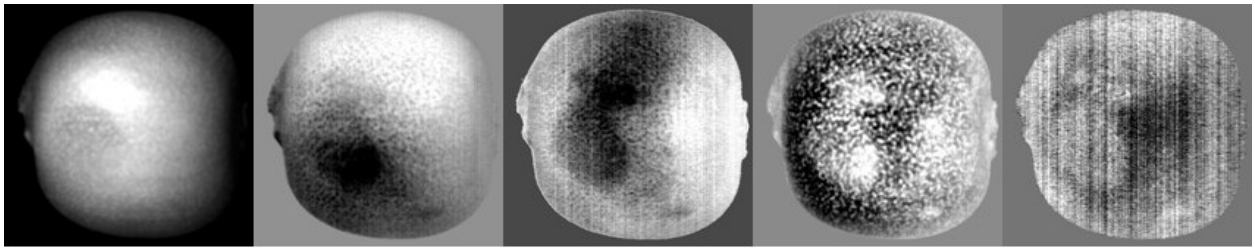

Figure 7. Principal component images obtained at the selected multiple wavelengths

obtained. In this sample, 100 pixels were observed as bruise, 100 pixels (50 pixels in the serious reflection area and 50 pixels in the other area) as normal. The pixels of these regions were used as the training set for SVM classifier. In this work, RBF kernel function was used for SVM. According to the principle of SVM, it is critical to determine the penalty parameter C and parameter γ of the kernel function, which impact directly on the final identification results. The best parameters of the training experiments (C = 100, γ = 0.3) were selected for RBF-SVM classification based on comparing the test results obtained for different values of the parameters.

In order to obtain a good performance, it is critical to determine the classification probability threshold, which impacts directly on the final identification results. After trying several options, some of the bruise region pixels remained unclassified when the classification probability threshold of 0.9 was used, but normal region pixels were classified correctly in this case. When the classification probability threshold was decreased to 0.7–0.6, almost all pixels of the bruise region were classified correctly. However, a number of normal region pixels were defined as the bruise region. The classification probability threshold of around 0.8 led to satisfactory classification results, although there were still a few normal region pixels. Consequently, the classification probability threshold of 0.8 was chosen as the threshold of SVM. The binary images of the bruise region obtained using SVM classifying and morphology processing such as hole filling and size filtering are shown in Figure 8.

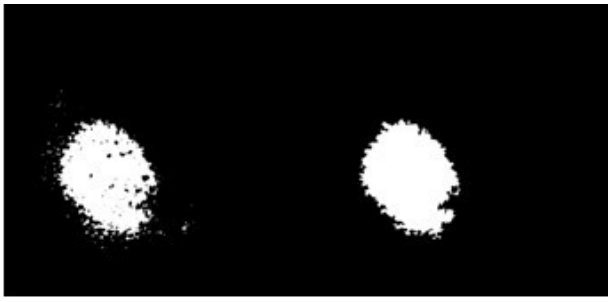

Figure 8. Results after (a) SVM classifying and (b) morphology processing

Bruise detection

The proposed system (including the hardware and algorithm) was used to test kiwifruits cv. Zhonghua. The results obtained are given in Table 1. The total error rate reached 12.5% occurring mostly in the bruise group, the positive error (normal fruits were classified as bruised fruits) was 15.6%, and the false error (bruised fruits were classified as normal fruits) was 8.8%. The transmission and reflection of the peel were inconsistent because of the existence of spots and rust on the surfaces of kiwifruits. So the rust and spot areas were segmented as bruise, which was the main reason for the positive error, and the main reason for the false error was the artificial injury on kiwifruit that was too moderate to allow segmentation.

Table 1. The results of hidden bruises detection on kiwifruits

Sample	Detection results	
	normal (91 fruits)	bruise (109 fruits)
Normal (100 fruits)	83	17
Bruise (100 fruits)	8	92
Classification error (%)	8.8	15.6
Global error (%)	12.5	

CONCLUSIONS

A Vis/NIR hyperspectral imaging system was developed to detect hidden bruises on kiwifruits in the wavelength range from 408 nm and 1117 nm. This system can acquire both spatial and spectral information from an object simultaneously. With the use of PCA, the high dimension spectral image data (wavelength range 600–900 nm) were reduced to images obtained at multiple optimal wavelengths of 682, 723, 744, 810, and 852 nm. An image processing algorithm using SVM for the component images of multiple waveband images was developed for determining whether kiwifruit was normal or bruised. The total detection error rate was 12.5%.

This study laid a foundation for further development of a computer vision system for the bruise detection on kiwifruits. Further research will focus on developing a more efficient multispectral imaging system, including a better classification algorithm and speeding up the data processing procedures to fulfill the goal of the real-time hidden bruise detection on kiwifruit.

References

Ariana D.P., Lu R.F., Guyer D.E. (2006): Near-infrared hyperspectral reflectance imaging for detection of bruises on pickling cucumbers. Computers and Electronics in Agriculture, **53**: 60–70.

Brosnan T., Sun D.W. (2004): Improving quality inspection of food products by computer vision – a review. Journal of Food Engineering, **61**: 3–16.

Byun H., Lee S.W. (2002): Applications of support vector machines for pattern recognition: a survey. In: Proceedings 1st International Workshop. SVM, Niagara Falls. USA.

Cao Q., Nagata M., Wang H., Bato P.M. (1999): Orientation and shape extraction of strawberry by colour image processing. In: 1999 ASAE Annual International Meeting, Paper No. 993161. St. Joseph, USA.

Guo L., Wu Y.X., Wu Q., Yan W.L., Shen X.Q. (2006): Research on automatic fingerprint classification based on support vector machine. In: Proceeding 6th World Congress on Intelligent Control and Automation, Dalian, China.

Kim S., Schatzki T.F. (2000): Apple watercore sorting using X-ray imagery: I. Algorithm development. Transactions of the ASAE, **43**: 1695–1702.

Leemans V., Magein H., Destain M.F. (1998): Defects segmentation on 'Golden Delicious' apples by using colour machine vision. Computers and Electronics in Agriculture, **20**: 117–130.

Liu Y.L., Chen Y.R., Wang C.Y., Chan D.E., Kim M.S. (2005): Development of a simple algorithm for the detection of chilling injury in cucumbers from visible/near-infrared hyperspectral imaging. Applied Spectroscopy, **59**: 78–85.

Liu Y.L., Windham W.R., Lawrence K.C., Park B. (2003): Simple algorithms for the classification of visible/near-infrared and hyperspectral imaging spectra of chicken skins, feces, and fecal contaminated skins. Applied Spectroscopy, **57**: 1609–1612.

Lu R., Chen Y.R., Park B., Choi K.H. (1999). Hyperspectralimaging for detecting bruises in apples. In: 1999 ASAE Annual International Meeting, Paper No. 993120. St. Joseph, USA.

Lu R. (2003): Detection of bruises on apples using near-infrared hyperspectral imaging. Transactions of the ASAE, **46**: 523–530.

Mehl P.M., Chen Y.R., Kim M.S., Chan D.E. (2004): Development of hyperspectral imaging technique for the detection of apple surface defects and contaminations. Journal of Food Engineering, **61**: 67–81.

Noh H.K., Lu R.F. (2007): Hyperspectral laser-induced fluorescence imaging for assessing apple fruit quality. Postharvest Biology and Technology, **43**: 193–201.

Park B., Lawrence K.C., Windham W.R., Smith D.P. (2006): Performance of hyperspectral imaging system for poultry surface fecal contaminant detection. Journal of Food Engineering, **75**: 340–348.

Park B., Windham W.R., Lawrence K.C., Smith D.P. (2007): Contaminant classification of poultry hyperspectral imagery using a spectral angle mapper algorithm. Biosystems Engineering, **96**: 323–333.

Paulus I., Schrevens E. (1999): Shape characterization of new apple cultivars by Fourier expansion of digital images. Journal of Agricultural Engineering Research, **72**: 113–118.

Qian H., Mao Y., Xiang W., Wang Z. (2010): Recognition of human activities using SVM multi-class classifier. Pattern Recognition Letters, **31**: 100–111.

Qin J., Burks T.F., Kim M.S., Chao K., Ritenour M.A. (2008): Citrus canker detection using hyperspectral reflectance imaging and PCA-based image classification method. Sensing and Instrumentation for Food Quality and Safety, **2**: 168–177.

Qin J., Burks T.F., Ritenour M.A., Bonn W.G. (2009): Detection of citrus canker using hyperspectral reflectance imaging with spectral information divergence. Journal of Food Engineering, **93**: 183–191.

Qin J., Lu R.F. (2007): Measurement of the absorption and scattering properties of turbid liquid foods using hyperspectral imaging. Applied Spectroscopy, **61**: 388–396.

Shahin M.A., Tollner E.W., Evans M.D., Arabnia H.R. (1999): Watercore features for sorting red delicious apples: a statistical approach. Transactions of the ASAE, **42**: 1889–1896.

Shahin M.A., Tollner E.W., Gitaitis R.D., Sumner D.R., Maw B.W. (2002a): Classification of sweet onions based on internal defects using image processing and neural network techniques. Transactions of the ASAE, **45**: 1613–1618.

Shahin M.A., Tollner E.W., McClendon R.W., Arabnia H.R. (2002b): Apple classification based on surface bruises using image processing and neural networks. Transactions of the ASAE, **45**: 1619–1627.

Thomas P., Kannan A. (1995): Non-destructive of weevil-infested mango fruits by X-ray imaging. Postharvest Biology and Technology, **5**: 161–165.

Throop J.A., Aneshansley D.J., Anger W.C., Peterson D.L. (2005): Quality evaluation of apples based on surface defects: development of an automated inspection system. Postharvest Biology and Technology, **36**: 281–290.

Vapnik V. (1998): Statistical Learning Theory. John Wiley and Sons Inc., New York.

Xing J., Baerdemaeker J.D. (2005): Bruise detection on 'Jonagold' apples using hyperspectral imaging. Postharvest Biology and Technology, **37**: 152–162.

Xing J., Bravo C., Jancsok P.T., Ramon H., Baerdemaeker J.D. (2005): Detecting bruises on 'Golden Delicious' apples using hyperspectral imaging with multiple wavebands. Biosystems Engineering, **90**: 27–36.

Xing J., Saeys W., Baerdemaeker J.D. (2007): Combination of chemometric tools and image processing for bruise detection on apples. Computers and Electronics in Agriculture, **56**: 1–13.

Received for publication March 4, 2010
Accepted after corrections November 16, 2010

Corresponding author:

Dr. Jian-rong Cai, Jiangsu University, School of Food & Biological Engineering, Xuefu Road 301, Zhenjiang City, Jiangsu Province, 212013, P.R. China
tel.: + 86 511 887 973 08, e-mail: jrcai66@gmail.com